# Adsorbate Vibrational Energies: Relation between Experiments and Rigid-Lattice Calculations

S. Andersson and P.-A. Karlsson
*Department of Physics, Chalmers University of Technology, S-41296 Göteborg, Sweden*

and

M. Persson
*Institute of Theoretical Physics, Chalmers University of Technology, S-41296 Göteborg, Sweden*

(Received 6 June 1983)

Experimental vibration spectra for ordered overlayers of O and S on Ni(100) are analyzed in terms of surface-lattice dynamics in relation to rigid-lattice calculations. It is shown how spectral differences for the consecutive $p(2\times 2)$ and $c(2\times 2)$ structures are primarily due to differences in the coupling to the substrate phonon modes.

PACS numbers: 68.30.+z, 68.20.+t

Vibration spectra of adsorbates on solid surfaces provide a most important source of information about the state of adsorption and possible adsorption geometries. Measured spectra are in general analyzed qualitatively, with use of selection rules, symmetry arguments, and empirical comparison of spectral features with data for suitable gauge substances. In some cases a direct comparison of measured and calculated vibrational energies has resulted in a determination of the adsorption geometry, e.g., for hydrogen adsorption on nickel surfaces, where vibrational energies derived from calculated potential curves[1,2] compare very favorably with those observed in electron-energy-loss measurements (EELS). For oxygen adsorption on Ni(100) a similar analysis has proven rather intricate. The unexpectedly large shift of the experimentally observed vibrational energies for oxygen in the consecutive $p(2\times 2)$ and $c(2\times 2)$ structures[3,4] has been suggested to be the consequence of a drastic change in the electronic structure of the adsorbate resulting in quite different oxygen positions, $d_\perp$, above the nickel surface.[1,5] This picture, however, is not supported by experimental structure investigations which rather yield $d_\perp \sim 0.8-0.9$ Å for both structures.[6-9] In this Letter we present EELS spectra for ordered overlayers of O and S on Ni(100) and discuss them in relation to rigid-lattice calculations. We show how spectral differences between the $p(2\times 2)$ and $c(2\times 2)$ O spectra are primarily due to the stronger coupling to substrate modes in the $p(2\times 2)$ case.

The Ni(100) specimen was cleaned by argon-ion bombardment and annealing according to standard procedures. The ordered O and S structures were formed and monitored by low-energy electron diffraction as described previously.[3] The EELS spectra were recorded at an ambient pressure of $2\times 10^{-11}$ Torr with use of a high-resolution electron spectrometer that has been described elsewhere.[10] The scattering plane containing the incident and the scattered electron beams is defined by the specimen surface normal and the [100] direction in the surface plane. The experimental spectra shown in Figs. 1 and 2 have been measured in the specular direction for an angle of incidence around 50° and an energy of the incident electrons around 2 eV. Angular measurements have been carried out routinely and show that the spectral features of interest are excited by dipole scattering, i.e., the loss intensity peaks sharply close to the specular direction.[10]

The experimental EELS spectra have been analyzed by a calculational scheme for lattice dynamics of dipole-active surface vibrational modes of a semi-infinite substrate.[11] The measured EELS spectrum is related to the spectral func-

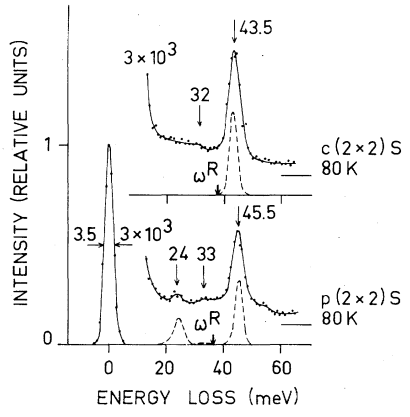


FIG. 1. EELS spectra for the $p(2\times 2)$S and $c(2\times 2)$S structures on Ni(100) and the corresponding spectral densities $g(\omega, \vec{r}^{\,*})$ (dashed curves) calculated for hollow-site adsorption and a sulfur distance, $d_\perp = 1.3$ Å, above the nickel surface.

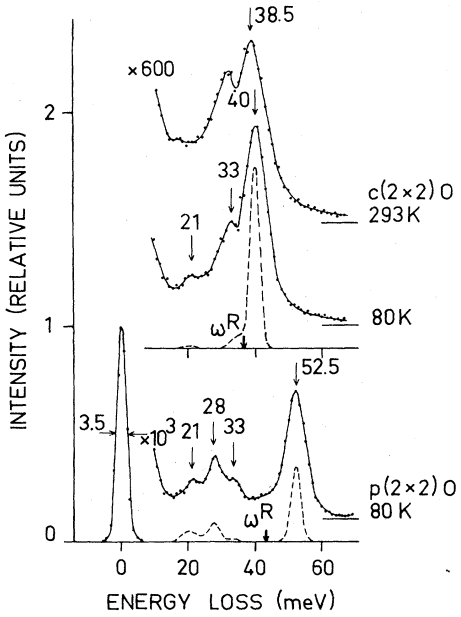


FIG. 2. EELS spectra for the $p(2\times 2)$O and $c(2\times 2)$O structures on Ni(100) and the corresponding spectral densities $g(\omega,\vec{\nu}^*)$ (dashed curves) calculated for hollow-site adsorption and an oxygen distance $d_\perp = 0.9$ Å above the nickel surface.

tion of displacements projected on the appropriate effective charge field $\vec{e}^*$. The symmetry of the adsorption site is introduced through the selection rule for dipole scattering which states that only totally symmetric displacement fields with respect to the symmetry group are dipole active for the ordered adsorbate lattices.[12] The differential cross section for dipole scattering is given by[13]

$$\frac{d^2\sigma}{d\Omega\, d(\hbar\omega)} = \frac{32me^2\pi^3}{\hbar^5\cos\alpha}\left|\frac{\vec{k}'}{\vec{k}}\right|\left|\left\langle\psi_{\vec{k}'}\left|\frac{z}{|\vec{x}|^3}\right|\psi_{\vec{k}}\right\rangle\right|^2 S(\vec{q},\omega), \quad (1)$$

where $\psi_{\vec{k}}, \psi_{\vec{k}'}$, are the wave functions of wave vectors $\vec{k}, \vec{k}'$ for the incident and scattered electron waves, respectively, $\alpha$ is the angle of incidence, $\hbar\vec{q} = \hbar\vec{k}_\parallel - \hbar\vec{k}_\parallel'$ is the surface component of the momentum transfer, and $\hbar\omega$ is the energy loss. $S(\vec{q},\omega)$ is the spectral dipole-dipole correlation function. The differential cross section given by Eq. (1) forms a narrow lobe that peaks close to the specular direction, i.e., close to the direction corresponding to $\vec{q}=0$. $S(\vec{q},\omega)$ can then be written as

$$S(\vec{q}=0,\omega) = N(e^{*2}\hbar/2M^*\omega)[1+\eta(\omega)]g(\omega,\vec{\nu}^*), \quad (2)$$

where $n(\omega)$ is the Bose-Einstein distribution factor, $N$ is the number of primitive cells, $M^*$ is the reduced mass, $e^*$ is the effective charge, and $g(\omega,\vec{\nu}^*)$ is the projected density of states

$$g(\omega,\vec{\nu}^*) = \sum_\kappa |(\vec{\xi}_\kappa\cdot\vec{\nu}^*)|^2\delta(\omega-\omega_\kappa); \quad (3)$$

$\omega_\kappa$ is the frequency of the eigenmode with the mass-weighted normalized displacement field $\vec{\xi}_\kappa$, and $\vec{\nu}^*$ is equal to the normalized mass-weighted effective charge field $\vec{e}^*$.

The experimental EELS spectra are compared with the spectral densities $g(\omega,\vec{\nu}^*)$ calculated with an appropriate force-constant model. We have found that a central nearest-neighbor force-constant model is adequate for our purpose. All parameters are determined from the maximum bulk phonon energy, the adsorbate position $d_\perp$, and the experimentally observed energy of the localized vibrational mode in the adsorbate layer. The shift of the overlayer mode, due to coupling to substrate vibrations, is determined from the energy $\hbar\omega^R$ of this mode, evaluated with the substrate atoms given infinite mass in the lattice-dynamical calculation. This corresponds to a rigid substrate lattice and $\hbar\omega^R$ is evidently also the relevant quantity for a comparison with vibrational energies obtained from potential-energy curves calculated for a rigid lattice.

Figures 1 and 2 summarizes the EELS spectra for the $p(2\times2)$ and $c(2\times2)$ structures of S and O on Ni(100) together with the corresponding calculated $g(\omega,\vec{\nu}^*)$. The experimental spectra have been recorded at 80 and 293 K specimen temperature. A general comparison of the experimental data for the two adsorbates reveals some striking differences. The oxygen frustrated translation shifts by 12.5 meV at 80 K (14 meV at 293 K) in going from $p(2\times2)$ to $c(2\times2)$ while the corresponding shift for sulfur is only 2 meV.

The dashed curves in Fig. 1 show the projected vibrational density of states, $g(\omega,\vec{\nu}^*)$, for the two S structures under the assumption of hollow-site adsorption and $d_\perp = 1.3$ Å as found in structural investigations.[6,7] The calculated $g(\omega,\vec{\nu}^*)$ has been broadened with a Gaussian of 3.5 meV width (full width at half maximum) in order to mimic the instrumental resolution. The $p(2\times2)$S EELS spectrum shows a peak at 24 meV which derives from the nickel surface phonon $S_6(\bar{X})$. The energy is substantially lowered, however, compared to that of the bare substrate and a 50% reduction of the force constant between the first and second Ni layers is required to bring the calculation into agreement with the experiment. The faint struc-

ture around 32–33 meV observed in both the $p(2\times2)$S and $c(2\times2)$S EELS spectra derives from one of the bulk subbands. This structure is, however, significantly weaker than in the corresponding O spectra, primarily because of the general reduction of the force constant between the first and second Ni layers in the sulfur case. For the rigid-substrate situation we find the sulfur frustrated translation energies to be $\hbar\omega^R = 36.5$ and 38 meV for the $p(2\times2)$S and $c(2\times2)$S structures, respectively, i.e., 9 and 5.5 meV lower than the observed energies. Upton and Goddard[1] obtained the vibrational energy 37 meV for S adsorbed in the hollow-site configuration on a rigid $Ni_{20}$ cluster which agrees very well with our $\hbar\omega^R$ values. The sulfur chemisorption state is evidently relatively insensitive to the specific adsorbate density.

The projected densities of states, $g(\omega,\vec{v}^*)$, for the corresponding oxygen structures were calculated under the assumption of hollow-site adsorption and $d_\perp = 0.9$ Å. The calculations reproduce the experimental spectra quite accurately (see Fig. 2). The peak at 28.5 meV in the $p(2\times2)$O EELS spectrum originates from the $S_6(\bar{X})$ mode[5,14,15] as for $p(2\times2)$S but is less shifted in this case. The fainter structures at 21 and 33 meV derive from the bulk subbands. The $c(2\times2)$ spectrum shows structure at 33 meV which derives from the bulk subband at $\bar{\Gamma}$.[5,14,15] This structure becomes more prominent at $T = 293$ K because of the increased coupling to the substrate phonon band as the oxygen mode shifts closer to the top of the band. The structure around 21 meV derives from the bulk subband at $\bar{M}$ and is reproduced in the calculated $g(\omega,\vec{v}^*)$ by an adsorbate-correlated alternating change in the force constant between the first and second Ni layers. Every second force constant has been weakened or strengthened by 50%. The oxygen frustrated translation energies for the rigid-substrate situation are found to be $\hbar\omega^R = 43.5$ and 37 meV for the $p(2\times2)$O and $c(2\times2)$O structures, respectively, i.e., 6 meV of the experimentally observed 12.5-meV energy difference is simply due to the stronger coupling to substrate modes in the $p(2\times2)$ case. This result is quite sensitive to the choice of $d_\perp$, e.g., for $d_\perp = 0.8$ Å we obtain $\hbar\omega^R = 42$ and 37 meV.

In Fig. 3 we have summarized how the energy shift, $\hbar\omega - \hbar\omega^R$, depends on the adsorbate structure, adsorbate position $d_\perp$, and adsorbate mass. A general feature seen in Fig. 3 is the larger energy shift for the heavier adsorbate in a given adsorbate structure. The larger shifts for the $p(2\times2)$ structures than for the $c(2\times2)$ structures are caused by the symmetry-allowed coupling, in the $p(2\times2)$ case, to substrate phonon states at the $\bar{X}$ point of the substrate surface Brillouin zone. This coupling is governed by $d_\perp$ and the shifts for the $p(2\times2)$ structures are consequently sensitive to $d_\perp$ as the results in Fig. 3 demonstrate. For the $c(2\times2)$ structures, on the other hand, the shifts are insensitive to $d_\perp$ and also to other details of the applied force-constant model as, e.g., noncentral components of the forces in the adsorbate structure or lateral interactions between the adsorbate atoms.

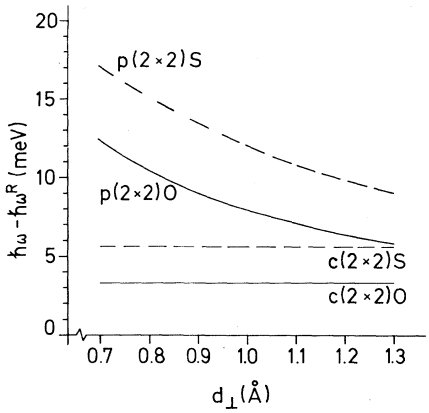


FIG. 3. Energy shifts $\hbar\omega - \hbar\omega^R$ of the O and S vibrational modes, for the $p(2\times2)$ and $c(2\times2)$ structures, calculated as a function of adsorbate position $d_\perp$, for hollow-site adsorption.

The oxygen loss peaks are substantially broader than the elastic peak and broaden further and shift when the specimen temperature is raised [see the $c(2\times2)$O spectra in Fig. 2]. Such a behavior is characteristic for anharmonic effects.[16,17] The sulfur spectra show minute broadening and temperature dependence which implies that the anharmonic coupling is weaker in this case, presumably because of a smaller root mean square amplitude of vibration.[16]

The oxygen mode energies are less than twice the maximum substrate phonon energy and we accordingly attribute the widths $2\Gamma$ of the oxygen loss peaks to two-phonon decay processes.[16] Deconvoluting the instrumental width of 3.5 meV we obtain from the 80-K spectra the intrinsic widths $2\Gamma = 5$ and 7 meV for the 52.5- and 40-meV loss peaks, respectively. The two-phonon decay processes also cause dynamical shifts $\Delta(\omega)$, intimately related to the widths $2\Gamma(\omega)$ via a causal-

ity (Kramers-Kronig) relation

$$\Delta(\omega)=\pi^{-1}\mathrm{P}\int_0^\infty d(\omega'^2)\,\Gamma(\omega')/(\omega^2-\omega'^2).$$

Using a simple Gaussian model for $\Gamma(\omega)$ adjusted to fit our observed widths we obtain dynamical shifts that through the energy dependence of $\Delta(\omega)$ contribute about 1.5 meV to the difference in the oxygen mode energies. There are other possible mechanisms that can shift the mode energy; e.g., dilation of the Ni lattice will give rise to a static shift.[16] We believe that this effect is partly responsible for the shift of the $c(2\times2)$O mode. We can presently, however, not make any quantitative estimate of its magnitude.

The resulting values for $\hbar\omega^R$, corrected for the dynamical shifts $\Delta(\omega)$, are 42 $[p(2\times2)\mathrm{O}]$ and 37 meV $[c(2\times2)\mathrm{O}]$ for $d_\perp=0.9$ Å and 40.5 and 37 meV for $d_\perp=0.8$ Å. The vibrational energies for the two oxygen chemisorption states that Upton and Goddard[1] identify in their rigid cluster calculations are 46 and 33 meV, i.e., a substantially larger difference than we arrive at. For $d_\perp$ in the range 0.8–0.9 Å, as observed in the structure determinations, we find that the change in the oxygen chemisorption state between the two structures is compatible with a vibrational energy shift of 3–5 meV. We conclude that the vibrational energy of an adsorbate in different structure situations can change appreciably because of structure-related differences in the coupling to the substrate vibrational modes.

We want to thank J. E. Demuth, J. K. Nørskov, and A. Sjölander for useful and stimulating discussions. This work was supported by the Swedish Natural Science Research Council.

[1]T. H. Upton and W. A. Goddard, III, Phys. Rev. Lett. 46, 1635 (1981).
[2]J. K. Nørskov, Phys. Rev. Lett. 48, 1620 (1982).
[3]S. Andersson, Solid State Commun. 20, 229 (1976), and Surf. Sci. 79, 385 (1979).
[4]S. Lehwald and H. Ibach, *Vibrations at Surfaces* (Plenum, New York, 1982), p. 137.
[5]T. S. Rahman, J. E. Black, and D. L. Mills, Phys. Rev. Lett. 46, 1469 (1981), and Phys. Rev. B 25, 883 (1982).
[6]J. E. Demuth, D. W. Jepsen, and P. M. Marcus, Phys. Rev. Lett. 31, 540 (1973).
[7]M. Van Hove and S. Y. Tong, J. Vac. Sci. Technol. 12, 230 (1975).
[8]J. Stöhr, R. Jaeger, and T. Kendelewicz, Phys. Rev. Lett. 49, 142 (1982).
[9]J. E. Demuth, N. J. DiNardo, and G. S. Cargill, III, Phys. Rev. Lett. 50, 1373 (1983).
[10]S. Andersson, *Vibrations at Surfaces* (Plenum, New York, 1982), p. 169.
[11]M. Persson, to be published.
[12]S. Andersson and M. Persson, Phys. Rev. B 24, 3659 (1981).
[13]See, e.g., H. Ibach and D. L. Mills, *Electron-Energy-Loss Spectroscopy and Surface Vibrations* (Academic, New York, 1982).
[14]G. Allan and J. Lopez, Surf. Sci. 95, 214 (1980).
[15]V. Bortolani, A. Franchini, F. Nizzoli, and G. Santoro, J. Electron Spectrosc. Relat. Phenom. 29, 219 (1983).
[16]See, e.g., A. A. Maradudin, in *Solid State Physics*, edited by F. Seitz and D. Turnbull (Academic, New York, 1966), Vol. 19.
[17]V. P. Zhdanov and K. I. Zamaraev, Catal. Rev. Sci. Eng. 24, 273 (1982).